REGULAR ARTICLE

blood advances

TRIM21 enhances bortezomib sensitivity in multiple myeloma by halting prosurvival autophagy

Jing Chen,* Wen Cao,* Xi Huang, Qingxiao Chen, Shuting Ye, Jianwei Qu, Yang Liu, Xing Guo, Shunnan Yao, Enfan Zhang, Jingsong He, Anqi Li, Li Yang, and Zhen Cai

Bone Marrow Transplantation Center, The First Affiliated Hospital, School of Medicine, Zhejiang University, Hangzhou, China

Key Points

- TRIM21 is associated with clinical significance in MM and can enhance the sensitivity of MM to bortezomib via autophage pathway.
- TRIM21 targets ATG5 directly and mediates ubiquitin-dependent ATG5 degradation in MM cells.

Bortezomib (bort) is an effective therapeutic agent for patients with multiple myeloma (MM); however, most patients develop drug resistance. Autophagy, a highly conserved process that recycles cytosol or entire organelles via lysosomal activity, is essential for the survival, homeostasis, and drug resistance in MM. Growing evidence has highlighted that E3 ligase tripartite motif–containing protein 21 (TRIM21) not only interacts with multiple autophagy regulators but also participates in drug resistance in various cancers. However, to date, the direct substrates and additional roles of TRIM21 in MM remain unexplored. In this study, we demonstrated that low TRIM21 expression is a factor for relapse in MM. TRIM21 knockdown (KD) made MM cells more resistant to bort, whereas TRIM21 overexpression (OE) resulted in increased MM sensitivity to bort. Proteomic and phosphoproteomic studies of TRIM21 KD MM cells showed that bort resistance was associated with increased oxidative stress and elevated prosurvival autophagy. Our results showed that TRIM21 KD MM cell lines induced prosurvival autophagy after bort treatment, suppressing autophagy by 3-methyladenine treatment or by the short hairpin RNA of autophagy-related gene 5 (*ATG5*)-restored–bort sensitivity. Indeed, ATG5 expression was increased and decreased by TRIM21 KD and OE, respectively. TRIM21 affected autophagy by ubiquitinating ATG5 through K48 for proteasomal degradation. Importantly, we confirmed that TRIM21 could potentiate the antimyeloma effect of bort through in vitro and in vivo experiments. Overall, our findings define the key role of TRIM21 in MM bort resistance and provide a foundation for a novel targeted therapeutic approach.

Introduction

Multiple myeloma (MM), a clonal expansion of antibody-secreting plasma cells throughout the bone marrow (BM), is the second most common hematologic malignancy worldwide.[1] The growing number of options of novel agents for treating MM have significantly improved the outcomes, which is particularly true for first-in-class proteasome inhibitors, such as bortezomib (bort). Bort-based treatment has been one of the most successful therapies for MM, but many patients still suffer from remissions and relapses until reaching a state of resistance characterized by shorter durations of clinical benefit.[2] Therefore, the exploration of new mechanisms for targeted agents that are highly efficacious in

Submitted 1 June 2022; accepted 9 April 2023; prepublished online on *Blood Advances* First Edition 21 April 2023. https://doi.org/10.1182/bloodadvances.2022008241.

*J.C. and W.C. contributed equally to this study.

The sequencing data are available via ProteomeXchange with identifier PXD042004.

Data are available on request from the corresponding author, Zhen Cai (caiz@zju.edu.cn).

The full-text version of this article contains a data supplement.

treating patients with relapsed/refractory MM is of paramount significance, especially if they can overcome the disadvantages of proteasome inhibitors and immunomodulatory drug resistance.

One of the mechanisms underlying bort resistance in MM is associated with the overexpression (OE) or mutations of the bort-binding pocket β5 proteasome subunit.[3] The elevated expression of proteins combating oxidative stress and posttranslational modifications, which mainly acts on tumor suppressors, has also been studied.[4,5] In addition, the interactions among growth factors, cytokines, and exosomes in BM and MM cells are thought to play an important role in MM drug resistance.[6] A recent study based on an integrated microarray gene expression profile found that an additional mechanism affecting MM resistance is autophagy.[7] This phenomenon occurs in various physiological and pathological cellular processes and acts as a double-edged sword in maintaining cellular homeostasis, either acting in a suppressive manner in some neurodegenerative diseases or promoting the survival of certain tumors.[8-10] Some studies have linked autophagy to the pathophysiology of MM, as the unfolded and misfolded proteins in MM are partially eliminated by autophagy to reach equilibrium.[11,12] With an improved understanding of autophagy in myeloma development, targeting the molecular mechanisms of autophagy may become a novel effective treatment option.

Ubiquitination has been demonstrated as essential for the autophagy process in organisms ranging from yeast to mammals. It occurs on autophagy-related genes (ATGs) and regulates their levels as well as their interactions with other proteins.[13] For example, the E3 ubiquitin protein ligase neural precursor cell expressed, developmentally downregulated 4 (NEDD4) is involved in regulating BECLIN1 via Lys11- and Lys63-linked ubiquitination in human HeLa cancer cells and promotes autophagy.[14] Moreover, BECLIN1 is ubiquitinated at Lys17 by tumor necrosis factor receptor–associated factor 6 (TRAF6) E3 ubiquitin protein ligase and triggers autophagy in mouse macrophages.[15]

Tripartite motif–containing protein 21 (TRIM21), another ubiquitin E3 ligase, is expressed universally in various cells owing to its indispensable physiological role, with its RING domain being responsible for ubiquitination. Studies have proved that TRIM21 can ubiquitinate IRF3, IRF5, IRF7, and IRF8 in specific circumstances. The precise mechanisms may be through the catalysis of K48- and K63-linked ubiquitination, thus targeting proteins for degradation through proteasome-mediated proteolysis.[16] The first study to show relevant TRIM21 involvement in autophagy indicated active IKKβ interaction with TRIM21, which resulted in the translocation of protein complex to autophagosomes for subsequent sequestration and degradation.[17] Consistently, a recent report observed that TRIM21 interacts with multiple regulators (ULK1, BECLIN1, and GABARAP) and receptors (sequestosome1/p62) of autophagy.[18] However, the link between TRIM21 and autophagy in MM pathobiology has not been investigated yet.

In this study, we discovered a reverse correlation of TRIM21 expression with MM relapse. We also found that TRIM21 knockdown (KD) activated autophagy and decreased bort-induced MM cell apoptosis via direct ATG5 ubiquitination. Furthermore, we demonstrated that TRIM21 KD–induced autophagy activation can be blocked by 3-methyladenine (3-MA) and shATG5 to restore sensitivity of MM cells to bort. These results provide insights into the development of new strategies for MM treatment.

Methods

Patients

After the acquisition of informed consent and approval by the Research Ethics Committee of the First Affiliated Hospital, College of Medicine, Zhejiang University, BM samples were obtained from 18 patients with MM. CD138+ MM cells were isolated from the BM using CD138 microbeads (Miltenyi Biotech, Bergisch Gladbach, Germany). The MM cell purity was tested to be 98% (>90%).

Cell lines and cell culture

The human MM cell lines JJN3, RPMI8226, and 293T were obtained from the Cell Bank of the Chinese Academy of Science; CAG, ARP-1, MM1R, MM.1S, U266, U266-Bort, and OPM2 cells were kindly provided by Qing Yi (Center for Hematologic Malignancy Research Institute, Houston Methodist). All MM cell lines were cultured in RPMI 1640 medium (Corning, NY) and 293T cells were grown in Dulbecco's Modified Eagle's medium (Corning, NY) supplemented with 10% heat–inactivated fetal bovine serum (FBS) (Thermo Fisher Scientific, Waltham, MA) at 37°C in humidified air containing 5% CO_2.

Reagents and antibodies

Primary antibodies to SSA1(TRIM21) were purchased from GeneTex International Corporation (San Antonio, TX) and Santa Cruz Biotechnology (Dallas, TX). CASP3, PARP, SQSTM1, LC3, ATG5, ATG7, ATG16L1, BCL2, BECLIN1, mTOR, pmTOR, and ER stress antibody sampler kit antibodies were obtained from Cell Signaling Technology (Boston, MA). ATG5 was purchased from Santa Cruz Biotechnology (Dallas, TX) and Cell Signaling Technology (Boston, MA). Flag, Ha, Ubiquitin, linkage-specific K48, and linkage-specific K63 antibody were obtained from Abcam (Cambridge, UK). Glyceraldehyde-3-phosphate dehydrogenase (GAPDH) was acquired from Santa Cruz Biotechnology (Dallas, TX). The other reagents used included 3-MA (Selleck, Houston, TX), MG-132 (Selleck, Houston, TX), bort (Selleck, Houston, TX), and Lipofectamine 2000 (Thermo Fisher Scientific, Waltham, MA).

Transfection

To obtain stable TRIM21 KD, green fluorescent protein-containing short hairpin RNA (shRNA) lentiviral particles targeting human *TRIM21* and a scrambled shRNA vector were designed and synthesized by Shanghai GenePharma Co, Ltd (Shanghai, China). For stable TRIM21 OE, lentiviral-*TRIM21* and ubiquitin ligase mutant–*TRIM21* were purchased from Shanghai Genechem Co, Ltd (Shanghai, China). For stable ATG5 KD, shRNA lentiviral particles targeting human *ATG5* and a scrambled shRNA vector were designed and synthesized by our own laboratory. The transfected MM cells were selected in culture media containing puromycin or neomycin (5 μg/mL) for 1 to 2 weeks. Puromycin or neomycin were purchased from Thermo Fisher Scientific (Waltham, MA).

RNA isolation and quantitative reverse transcription polymerase chain reaction (qRT-PCR) analysis

Total RNA was isolated from MM cells using TRIzol (Invitrogen,Waltham, MA) according to the manufacturer's instructions. For messenger RNA dosage evaluation, complementary DNA was synthesized using the PrimeScript RT Reagent Kit with gDNA Eraser (Takara, Kyoto, Japan), and quantitative PCR was performed

to detect *TRIM21* levels by using the iTaq Universal SYBR Green Supermix (Bio-Rad, Hercules, CA). Relative expression was calculated using the comparative threshold cycle (Ct) method, and *GAPDH* served as an internal control. The experiments were carried out in triplicate and the primer sequences were as follows: *TRIM21* (forward 5'- TCAGAGCTAGATCGAAGGTGC-3'; reverse 5'- ACTCACTCCTTTCCAGGACAAT-3') and *GAPDH* (forward 5'-ACGGATTTGGTCGTATTGGGC-3'; reverse 5'-ACGGATTTGGTCGTATTGGGC-3').

Western blot analysis

The cells were harvested and extracted using RIPA buffer (SIGMA,Saint Louis, MO) containing a mixture of protease and phosphatase inhibitor (Thermo Fisher Scientific,Waltham, MA). Protein concentration was determined using a BCA Protein Assay Kit (KeyGEN BioTECH, Nanjing, China). Protein extracts (20-40 μg) were separated by 4% to 12% and 12% of SDS-polyacrylamide gel electrophoresis and then transferred to polyvinylidene difluoride membranes (Merck Millipore, Darmstadt, Germany). After blocking in 5% of nonfat milk (BD, Franklin, NJ) or 5% of bovine serum albumin for 1 to 2 hours, the membranes were incubated with primary antibodies at 4°C overnight, followed by the corresponding HRP-conjugated anti-rabbit or anti-mouse secondary antibodies (GeneScript, Nanjing, China). The signals were detected using an enhanced chemiluminescence detection kit (Biological Industries, Kibbutz Beit Haemek, Israel) and the ChemiDoc MP Imaging System (Bio-Rad, Hercules, CA).

Phosphokinase array

The Bort-induced protein phosphorylation of shTRIM21 and shNC MM1R were determined using the Human Phospho-Kinase Array Kit (R&D System, Hinnerup, Denmark). The spots were quantified using the ChemiDoc MP Imaging System (Bio-Rad, Hercules, CA), and the values were expressed as optical density units.

Reactive oxygen species (ROS)

ROS production in MM cells with or without bort treatment was analyzed using the CellROX Oxidative Stress Reagent (Thermo Fisher Scientific, Waltham, MA).

Immunofluorescence-confocal laser-scanning microscopy

The TRIM2 KD and TRIM21 OE MM stable cells were fixed with 4% paraformaldehyde, permeabilized with 0.5% Triton X-100 and incubated first with the indicated primary antibodies and then with the secondary antibodies. The nuclei were counterstained with 4′,6-diamidino-2-phenylindole. LC3-II puncta formation was detected by taking images using a confocal fluorescence microscope.

Analysis of cell viability and apoptosis

Cell viability was assayed using a Cell Counting Kit-8 (CCK-8) (Dojindo, Kyushu, Japan). Briefly, MM cells (5×10^3/100 μL per well) treated with different concentrations of bort were seeded in triplicate in 96-well plates at 37°C. After the indicated times, cell viability was evaluated by CCK-8 assay according to the manufacturer's instructions. To assess cell apoptosis, MM cells (1×10^5/mL per well) with the indicated treatments were seeded in 12-well plates at 37°C. After the indicated times, annexin V and proteasome inhibitor double staining was performed using an annexin V, FITC Apoptosis Detection Kit and annexin V, 633 Apoptosis Detection Kit (Dojindo, Kyushu, Japan) according to the manufacturer's instructions. The cells were measured using flow cytometry (BD Biosciences, San Diego, CA) and analyzed with FlowJo X 10.0.7.

Co-IP and in vivo ubiquitination assay

To immunoprecipitate the endogenous proteins, protein A/G magnetic beads (Thermo Fisher Scientific, Waltham, MA) were used to preclear the whole-cell extracts, followed by overnight incubation with the relevant antibodies and immunoglobulin G at room temperature. The beads were washed 3 times with lysis buffer using the Dynabeads Co-Immunoprecipitation Kit according to the manufacturer's instructions (Thermo Fisher Scientific, Waltham, MA), and the immunoprecipitation complexes were subjected to SDS-PAGE. To detect ATG5 ubiquitination, FLAG-tagged TRIM21 was designed and cloned to the GV341 expression vector, and the HA-tagged ATG5 and HIS-tagged Ubiquitin were designed and cloned to the GV219 expression vector using Shanghai Genechem Co, Ltd, then cotransfected into 293T cells by Lipofectamine 2000 (Thermo Fisher Scientific, Waltham, MA) . After 6 hours, the transfected cells were placed into new Dulbecco's Modified Eagle's medium containing 10% FBS. After 24 hours, DMSO or 25 μm MG-132 were added to 293T cells for 6 hours. Next, 293T cells were lysed in RIPA buffer containing an additional 1% SDS, then heated at 120°C for 5 minutes to dissociate the protein complexes. The heated lysates were diluted using 10× volume of RIPA buffer. ATG5 or Ub were immunoprecipitated from the cell lysates after incubating the antibodies with Dynabeads, and the samples were subsequently blotted with antibodies.

Statistical analysis

All data were expressed as the mean ± standard deviation of at least 3 independent experiments performed in triplicate. Student *t* test was used to estimate the statistical significance of differences using GraphPad Prism 6.0 software (GraphPad Software). *P* values <.05 were considered as statistically significant (*$P < .05$, **$P < .01$, ***$P < .001$).

Results

TRIM21 is associated with clinical significance in MM

To assess the expression status of TRIM21 in MM, we first examined TRIM21 expression in 9 MM cell lines (MM1R, MM.1S, JJN3, ARP-1, U266, U266-Bort, OPM2, RPMI8226, and CAG) and peripheral blood mononuclear cells from 1 healthy donor using qRT-PCR and western blot. As shown in Figure 1A -B, TRIM21 was expressed universally in all detected MM cell lines. MM1R and MM.1S exhibited higher expression among these 9 MM cell lines, whereas JJN3 and ARP-1 had relatively low expression. We further examined TRIM21 expression in BM samples obtained from the 18 patients with MM and found that TRIM21 levels were higher in patients with newly diagnosed MM than those in the same patients with relapsed MM treated with bort-based regimen using immunohistochemistry (Figure 1C-D). We also identified TRIM21 in CD138+ MM cells from the BM biopsies of patients with MM using immunofluorescence (supplemental Figure 1) and found that TRIM21 was decreased in RRMM. In addition, we searched the public data sets for MM and GSE9782 showed that elevated

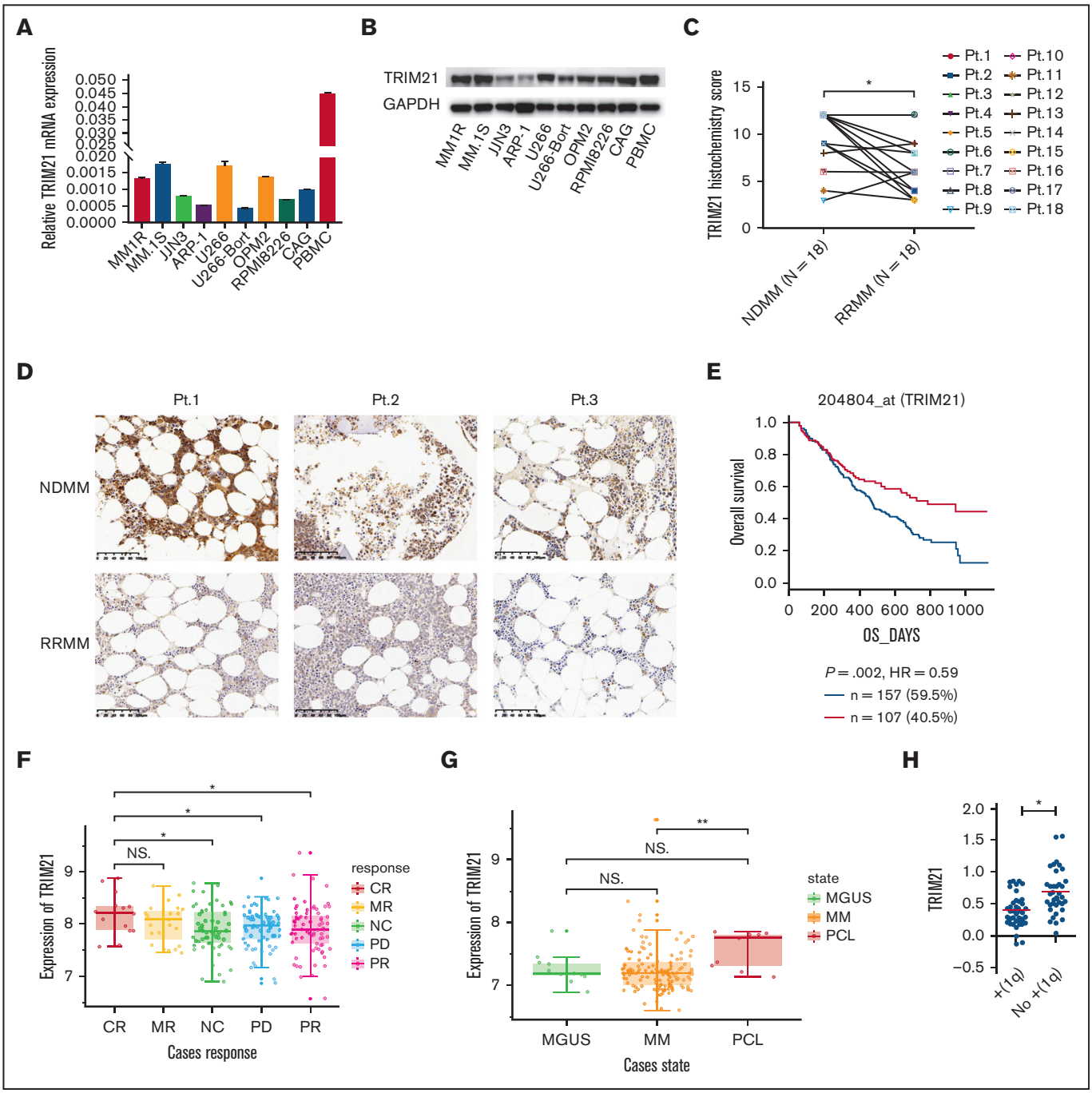

Figure 1. TRIM21 downregulation is associated with a high relapse rate in human MM. (A) qRT-PCR and (B) western blot analysis of TRIM21 expression in 9 MM cell lines (MM1R, MM.1S, JJN3, ARP-1, U266, U266-Bort, OPM2, RPMI8226, and CAG) and peripheral blood mononuclear cells (PBMCs) from 1 healthy donor. (C) The histochemistry score for TRIM21 was evaluated using BM biopsy samples when the patients were newly diagnosed and relapsed after treatment with a bort-based regimen (median H-score from 9.222222 to 6.388889). Pt.1 to Pt.18 represent 18 independent patients. (D) Immunohistochemical analysis of TRIM21 expression in 3 representative BM biopsies (Pt.1-Pt.3). The top panel shows TRIM21 expression in newly diagnosed patients, and the bottom panel shows TRIM21 expression after the relapse of the same patients after treatment with a bort-based regimen. Scale bars; 100 μm. (E) Kaplan-Meier survival analysis in the indicated myeloma data sets. Patients were divided into 2 groups based on *TRIM21* expression levels (red curve: high *TRIM21* expression; blue curve: low *TRIM21* expression). (F) *TRIM21* expression according to bort response (CR, n = 14; MR, n = 23; NC, n = 60; PD, n = 66; PR, n = 76). (G) *TRIM21* expression in the CD138+ plasma cells of patients with monoclonal gammopathy of undetermined significance (MGUS, n = 7), MM (n = 39), and plasma cell leukemia (PCL, n = 6). The y-axis indicates the median log value of *TRIM21* retrieved from the original data set. (H) MM patients with 1q amplified chromosomal abnormalities have low TRIM21 expression according to qRT-PCR detection. (*$P < .05$; **$P < .01$; ***$P < .001$).

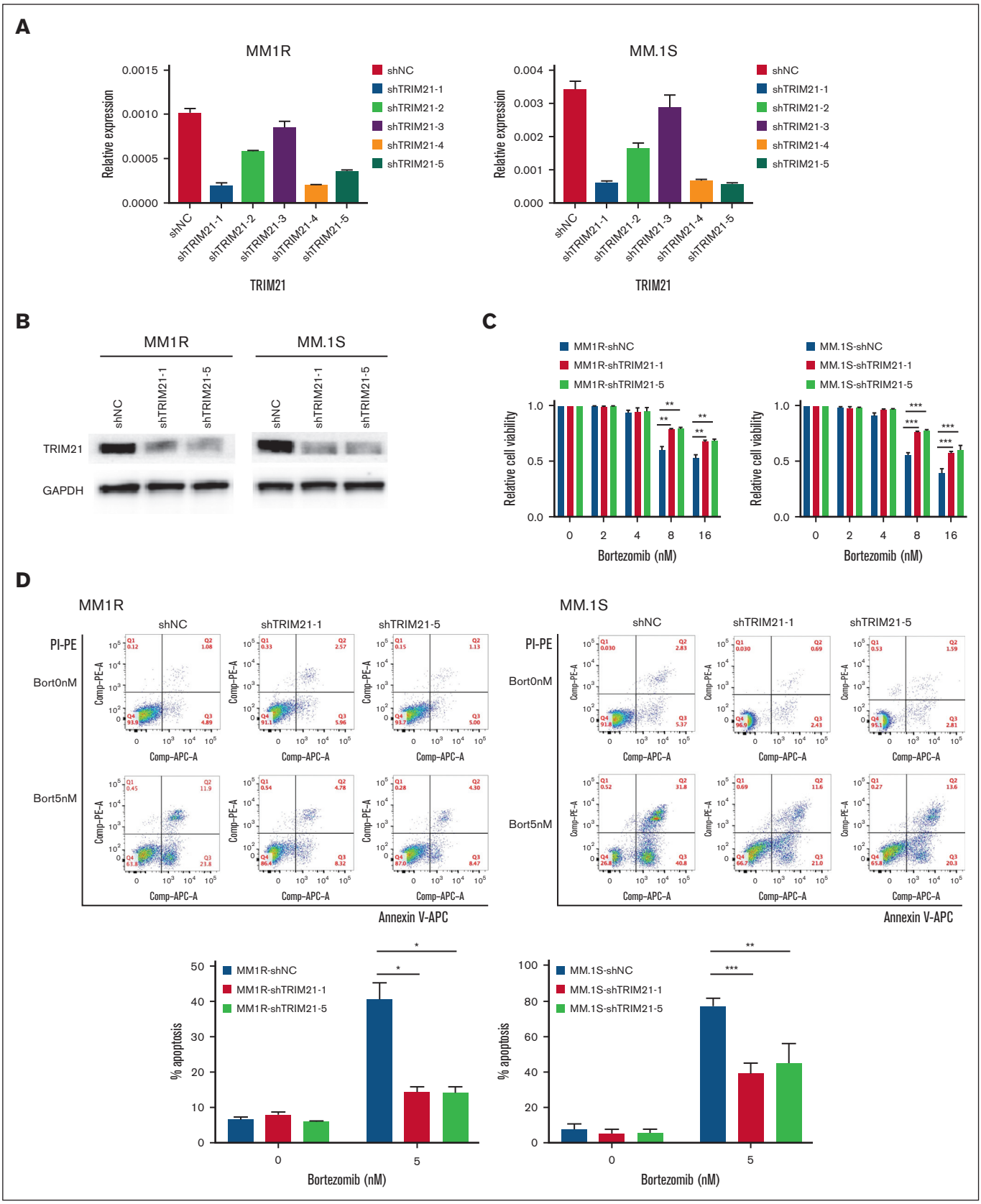
A
MM1R
MM.1S
Relative expression
shNC
shTRIM21-1
shTRIM21-2
shTRIM21-3
shTRIM21-4
shTRIM21-5
TRIM21
B
MM1R
MM.1S
TRIM21
GAPDH
C
MM1R-shNC
MM1R-shTRIM21-1
MM1R-shTRIM21-5
MM.1S-shNC
MM.1S-shTRIM21-1
MM.1S-shTRIM21-5
Relative cell viability
Bortezomib (nM)
D
MM1R
MM.1S
PI-PE
Bort0nM
Bort5nM
Comp-PE-A
Comp-APC-A
Annexin V-APC
% apoptosis
Bortezomib (nM)

Figure 2.

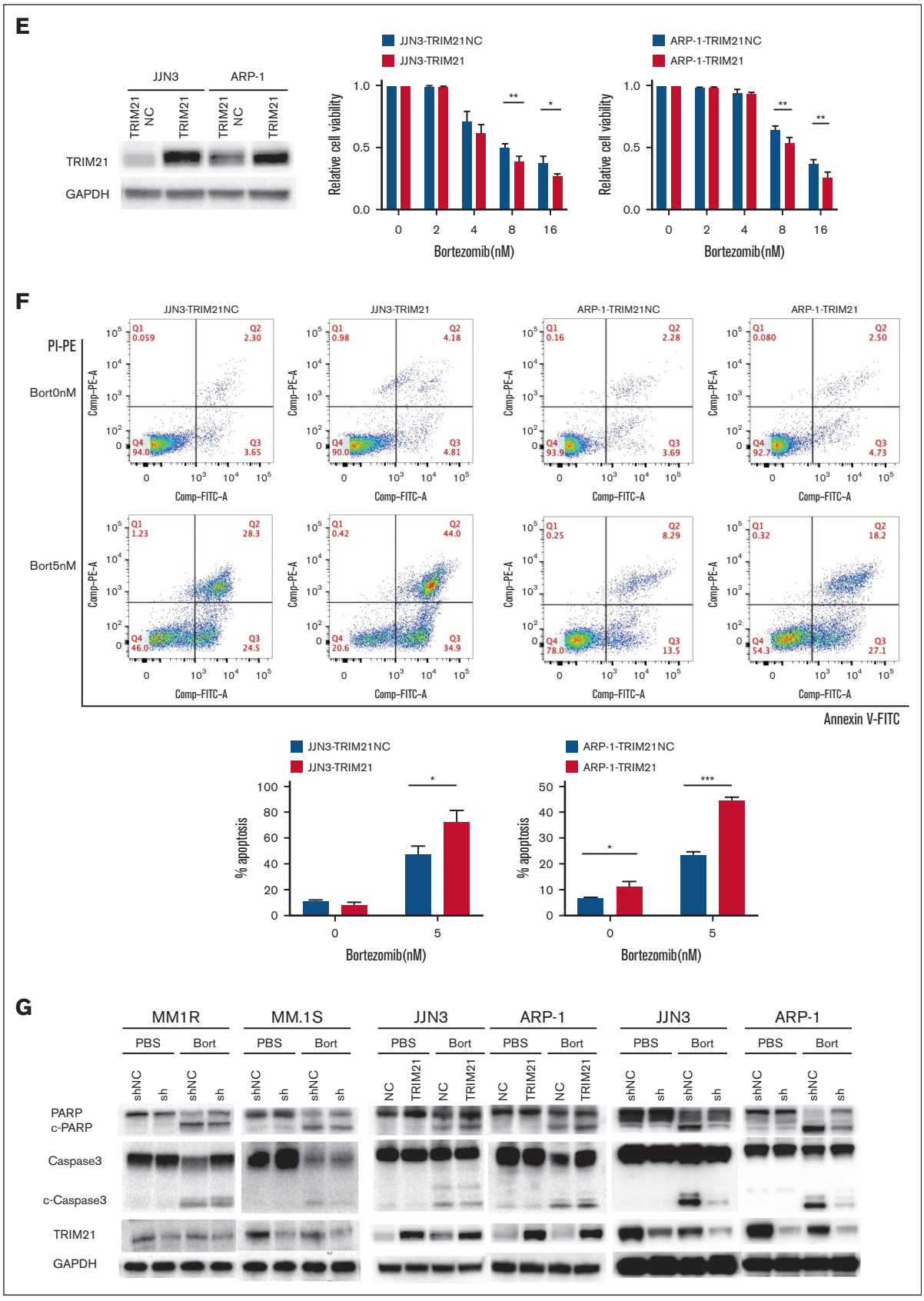

Figure 2 (continued)

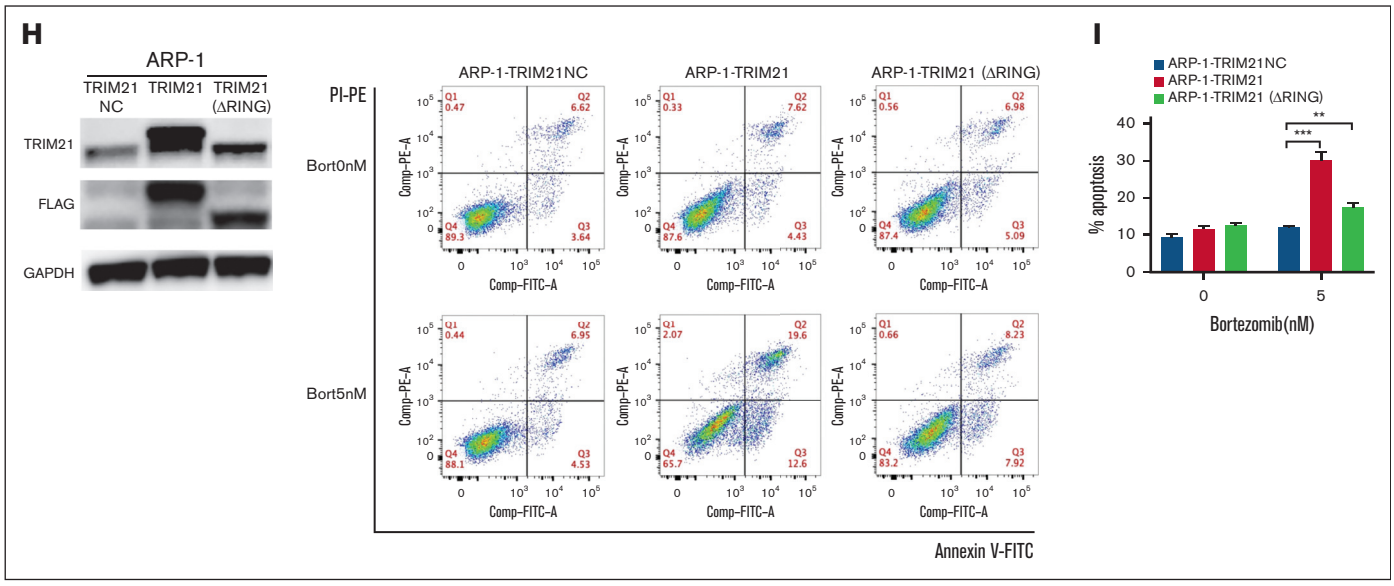

Figure 2 (continued) TRIM21 enhances the anti-MM activity of bort. (A) MM1R and MM.1S cells were lentivirally transduced with shNC and shTRIM21 (1, 2, 3, 4, and 5). qRT-PCR was performed to verify the transfection efficiency. (B) Western blot assay of MM1R and MM.1S cells lentivirally transduced with shNC and shTRIM21 (1 and 5). The TRIM21 and GAPDH protein levels are shown. (C) CCK-8 assay of MM1R and MM.1S cells lentivirally transduced with shNC or shTRIM21 (1 and 5) and treated with different concentrations of bort. (D) MM1R and MM.1S cells lentivirally transduced with shNC and shTRIM21 (1 and 5) were cultured in the absence or presence of bort (5 nM for both cells; 24 hours). Apoptosis was evaluated using flow cytometry with Annexin-V-APC/proteasome inhibitor (PI)-PE staining. The representative and summarized results show that TRIM21 KD prevents bort-induced apoptosis of MM1R and MM.1S cells. (E) Western blot assay and CCK-8 assay of JJN3 and ARP-1 cells transduced with TRIM21NC and TRIM21 and treated with different concentrations of bort. (F) Flow cytometry assay of JJN3 and ARP-1 cells transduced with TRIM21NC and TRIM21 in the absence or presence of bort (5 nM for both cells; 24 hours). The representative and summarized results show that TRIM21 OE increased bort-induced apoptosis. (G) Stable transfected MM cells were treated with phosphate-buffered saline (PBS) or bort for 24 hours and then lysed and extracted. Western blotting was performed to detect the expression levels of the PARP and Caspase-3 (as reflected by apoptosis). GAPDH was used as a loading control. (H) FALG-TRIM21 and FALG-TRIM21(△RING) were overexpressed in ARP-1 cells, which were then treated with bort (0 and 5 nmol/L) for 24 hours and detected using flow cytometry. (I) The summarized results show the percentage of cells undergoing apoptosis. The values are presented as the mean ± standard deviation (SD) of 3 independent experiments. (*$P < .05$; **$P < .01$; ***$P < .001$).

TRIM21 expression was associated with higher overall survival (Figure 1E) and patients with MM showed a response to bort (Figure 1F). GSE13591 revealed that *TRIM21* expression was higher in plasma cell leukemia than in MM, suggesting that *TRIM21* was positively correlated with myeloma aggressiveness (Figure 1G). Using the Agnelli myeloma database, we found a significant negative correlation between *TRIM21* and 1q-amplified chromosomal abnormalities (Figure 1H). Bort could effectively treat patients with MM with high-risk chromosomal abnormalities, such as del(17p), t (4,14), t (14;16); however, it could not improve the prognosis of patients with 1q21 amplification, suggesting that TRIM21 may play a role in MM bort resistance. Collectively, these findings indicate that low TRIM21 expression in MM cells may be a risk factor for MM.

TRIM21 enhances the anti-MM activity of bort

Aiming to define the effect of TRIM21 on MM cell sensitivity to bort, MM1R and MM.1S cells were lentivirally transduced with shNC and shTRIM21(1, 2, 3, 4, 5). By performing qRT-PCR, we observed that sequences 1 and 5 conferred the best transfection efficiency at the messenger RNA level (Figure 2A). We further confirmed the effect of sequences 1 and 5 using western blotting at the protein levels (Figure 2B). We measured cell viability using the Cell Counting Kit-8 (CCK-8) at 24 hours. As shown in Figure 2C, cell viability was significantly increased in high-dose–bort-treated groups in shTRIM21 (1,5)-transfected MM1R and MM.1S cells compared with shNC transfection, indicating that TRIM21 KD conferred higher bort resistance to MM cells. Moreover, we examined whether apoptotic events were affected in cells transfected with shTRIM21(1, 5) using flow cytometry assay. As shown in Figure 2D, TRIM21 KD decreased bort-induced apoptosis in MM1R and MM.1S cells. Simultaneously, we performed CCK-8 assays and flow cytometry to analyze the cell viability and apoptosis among the TRIM21 OE and TRIM21 NC MM cell lines (JJN-3 and ARP-1) treated with different concentrations of bort for 24 hours. As shown in Figure 2E-F, TRIM21 OE led to decreased cell viability and otherwise increased apoptosis compared with the control transfections. Furthermore, the TRIM21-induced apoptotic events were associated with the activation of cleaved PARP and Caspase 3 (Figure 2G). We also found that the increased sensitivity of MM cells to bort caused by TRIM21 was associated with E3-ligase ubiquitinase activity, as shown in Figure 2H-I; a ligase-dead mutant Flag-TRIM21 (RING domain delete, △RING) failed to increase the sensitivity of ARP-1 cells to bort. These data revealed that TRIM21 OE increased the sensitivity of MM cells to bort.

TRIM21 mediates proteomic and phospho-proteomic changes

To screen for proteins associated with bort resistance, we conducted the quantitative proteomics analysis of shTRIM21-MM1R and shNC-MM1R cells. Downregulated and upregulated proteins in TRIM21 KD MM1R cells were subjected to analysis against the

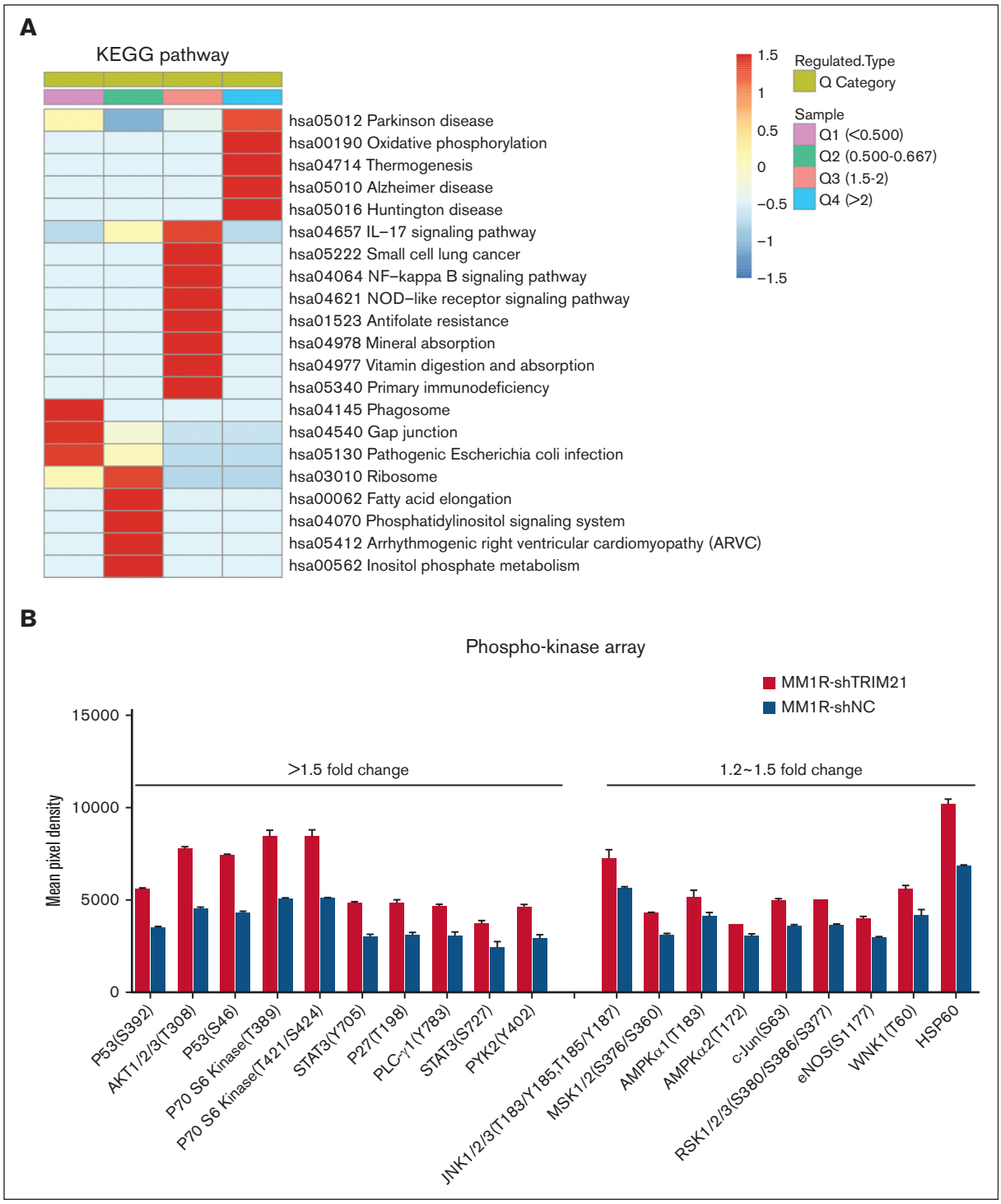

Figure 3. Proteomics and phospho-proteomics analysis of TRIM21 KD MM cells. (A) Quantitative proteomics analysis of MM1R-shNC and MM1R-shTRIM21 cells. We defined the differentially modifieed protein sites of shTRIM21/ shNC MM1R cells into Q1 to Q4 according to change levels. Q1: upregulated by more than twofold, Q2: upregulated by 1.5-2 –fold, Q3: downregulated by 1.5-2 –fold, Q4: downregulated by more than twofold. Kyoto Encyclopedia of Genes and Genomes (KEGG) pathway enrichment analysis of differentially expressed proteins: red indicates significant enrichment, blue indicates nonsignificant enrichment. (B) Effect of bort (5 μM; 24 hours) on the phospho-proteome profile of MM1R-shNC and MM1R-shTRIM21 cells according to a human phosphokinase array. The results are expressed as the mean pixel density. The histograms show that the 19/43 phospho-proteins are differentially expressed following bort treatment. The values are presented as mean ± SD. (*$P < .05$; **$P < .01$; ***$P < .001$).

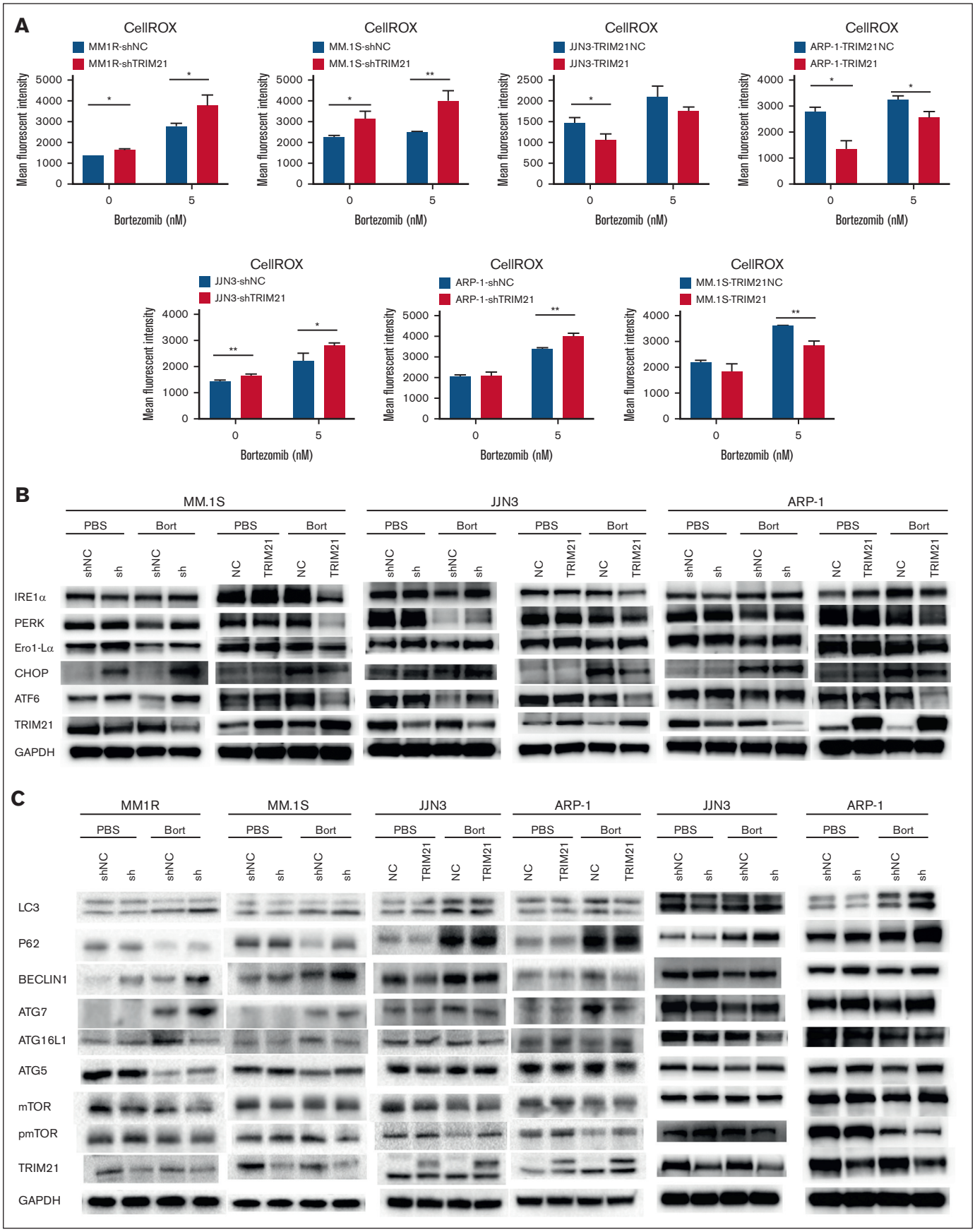
A
CellROX
MM1R-shNC
MM1R-shTRIM21
Mean fluorescent intensity
Bortezomib (nM)
CellROX
MM.1S-shNC
MM.1S-shTRIM21
CellROX
JJN3-TRIM21NC
JJN3-TRIM21
CellROX
ARP-1-TRIM21NC
ARP-1-TRIM21
CellROX
JJN3-shNC
JJN3-shTRIM21
CellROX
ARP-1-shNC
ARP-1-shTRIM21
CellROX
MM.1S-TRIM21NC
MM.1S-TRIM21
B
MM.1S
JJN3
ARP-1
PBS
Bort
shNC
sh
NC
TRIM21
IRE1α
PERK
Ero1-Lα
CHOP
ATF6
TRIM21
GAPDH
C
MM1R
MM.1S
JJN3
ARP-1
LC3
P62
BECLIN1
ATG7
ATG16L1
ATG5
mTOR
pmTOR
TRIM21
GAPDH

Figure 4.

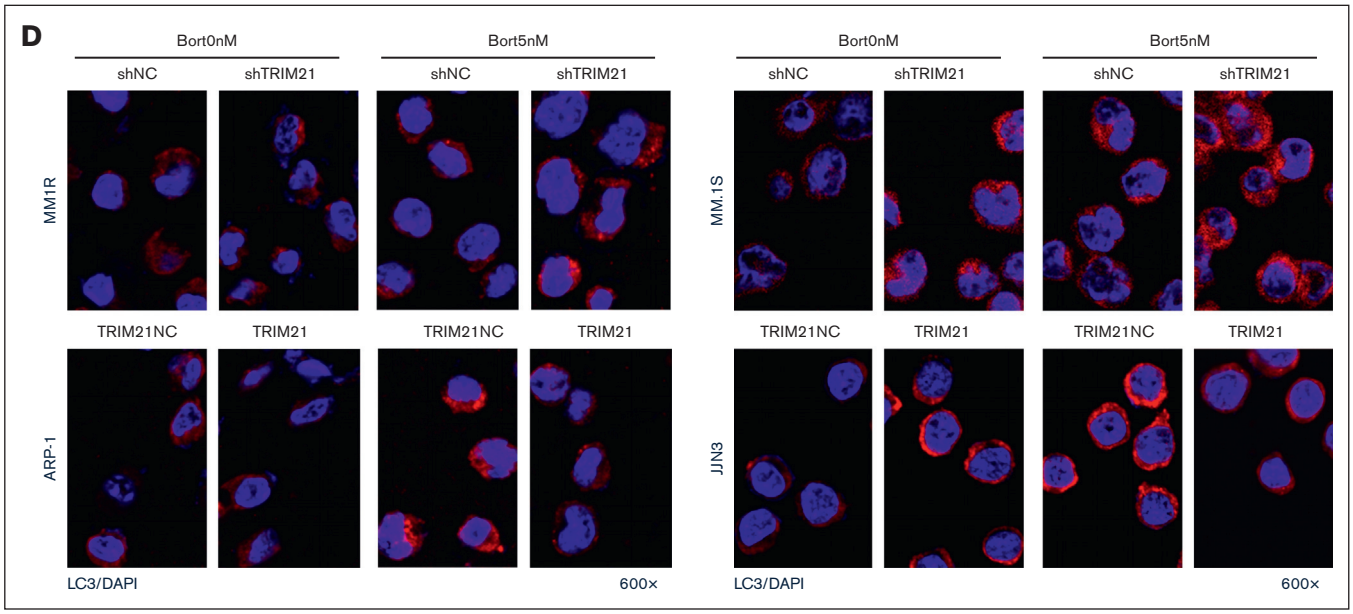

Figure 4 (continued) Bort activates prosurvival autophagy in TRIM21 KD MM cell lines. (A) Flow cytometry assay of total ROS expression of TRIM21 KD and TRIM21 OE MM1R, MM.1S, JJN3 and ARP-1 in the absence or presence of bort (5 nM; 24 hours). (B) Western blot analysis of IRE1α, PERK, Ero1-Lα, CHOP, and ATF6 proteins in TRIM21 KD, TRIM21 OE, and negative control MM cells, either untreated or treated with bort (5 nM, 24 hours). GAPDH was used as a loading control. (C) Western blot analysis of p62 and LC3 proteins (as autophagy markers), ATG5, ATG7, and ATG16L1 proteins (ATGs), and mTOR and p-mTOR in TRIM21 KD, TRIM21 OE, and negative control MM cells, either untreated or treated with bort (10 nM, 24 hours). GAPDH was used as a loading control. (D) Immunofluorescence assay of LC3 expression in TRIM21 KD, TRIM21 OE, and negative control MM cells in the absence or presence of bort. LC3-II expression is indicated by the strong red puncta. Original magnification: 600×, scale bar: 50 μm. The values are presented as the mean ± SD from 3 independent experiments. (*$P < .05$; **$P < .01$; ***$P < .001$).

Kyoto Encyclopedia of Genes and Genomes database. Our results revealed that the proteins (shTRIM21/shNC) that were upregulated by more than twofold were enriched mainly in the hsa00190 oxidative phosphorylation pathway, whereas those downregulated by more than twofold were mainly enriched in the hsa04145 phagosome pathway (Figure 3A). These results highlighted the possible role of TRIM21 in cellular stress and autophagy. Consistently, we examined the phosphorylation status of 43 proteins in shTRIM21-MM1R and shNC-MM1R cells in the presence of bort, and the results showed that shTRIM21-MM1R significantly increased the phosphorylation of HSP60, c-Jun, and p53 (cell stress markers) as well as the phosphorylation of the autophagy-associated protein P70S6Kinase (autophagy activator), as compared with shNC-MM1R cells (Figure 3B).

TRIM21 KD MM cells show cellular stress and activated autophagy after bort treatment

To verify the proteomics results, we examined whether TRIM21 could affect cellular stress and autophagy in MM cells. For cellular stress, we performed flow cytometry analysis to evaluate cellROX (Figure 4A) expression, which reflected the total ROS. Compared with control cells, TRIM21 KD MM cells produced higher levels of ROS, which increased in the presence of bort, and TRIM21 OE MM cell lines had a lower production of total ROS than the control groups. As seen in Figure 4B, western blotting showed that TRIM21 KD activated the ER stress pathway, whereas TRIM21 OE suppressed ER stress signal under bort treatment. TRIM21 has been proposed as a platform for autophagic regulatory factor assembly in a study reconstructing TRIM-mediated–precision autophagy.[18] Considering the role of bort in ER stress exacerbation, endogenous ROS production, and autophagy induction, we wondered whether bort resistance induced in TRIM21 KD MM cell lines activated autophagy to promote cell adaptation and survival. Thus, we performed western blotting to analyze LC3-II conversion, p62 degradation (an autophagy cargo receptor protein), and a series of essential autophagy genes. LC3-I is converted to LC3-II by proteolytic cleavage and lipidation, and it translocates to the surface of autophagy-specific intracellular vesicles during autophagy. To avoid autophagy activation induced by starvation, TRIM21 KD MM cell lines were treated with bort in the presence of 10% FBS. As shown in Figure 4C, TRIM21 KD caused an obvious increase in LC3-I conversion to LC3-II and a decrease in p62 degradation. ATG5, ATG7, and BECLIN1 expressions were also enhanced. Immunofluorescence staining of bort-treated TRIM21 KD MM cell lines showed strong punctuate dots (Figure 4D), implying the accumulation and translocation of LC3-II to autophagosomes. Further confirmation of activated autophagy was detected using electron microscopy. TRIM21 KD and U266-bort markedly increased identified autophagic vacuoles numbers per cell following incubation in 3-MA with bort treatment (supplemental Figure 3).

Next, we aimed to further confirm the function of TRIM21 function in autophagy. We used TRIM21 OE MM cell lines (JJN-3, ARP-1) to repeat the above-mentioned validation assays to examine whether TRIM21 OE had the opposite effect. Western blot analysis showed that TRIM21 OE reduced conversion to LC3-II and ATG5, ATG7, and BECLIN1 expression but increased p62 degradation upon bort treatment (Figure 4C). Moreover, the immunofluorescence

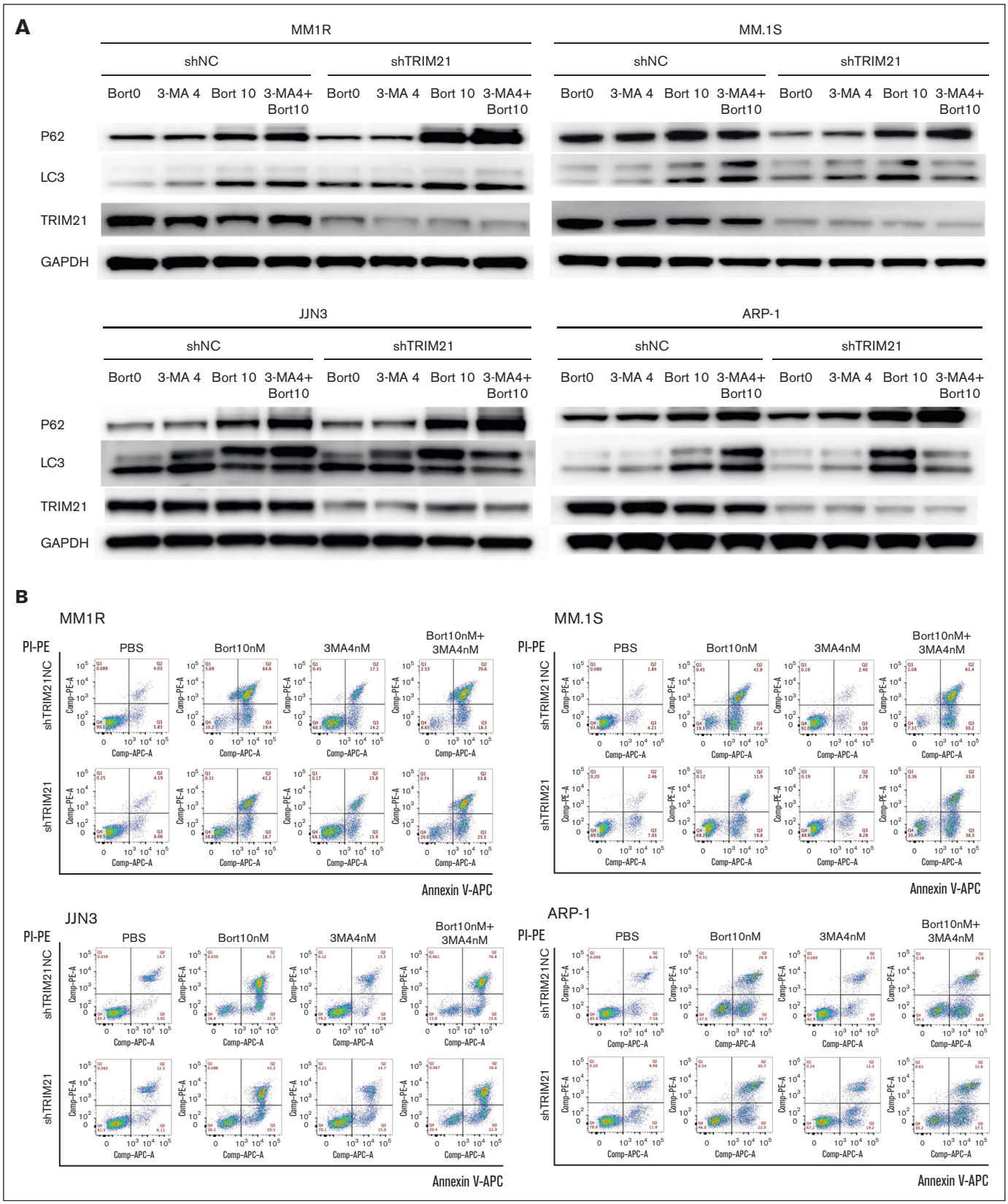
A
MM1R
MM.1S
shNC
shTRIM21
Bort0
3-MA 4
Bort 10
3-MA4+ Bort10
P62
LC3
TRIM21
GAPDH
JJN3
ARP-1
B
MM1R
MM.1S
JJN3
ARP-1
PI-PE
PBS
Bort10nM
3MA4nM
Bort10nM+ 3MA4nM
shTRIM21NC
shTRIM21
Comp-PE-A
Comp-APC-A
Annexin V-APC

Figure 5.

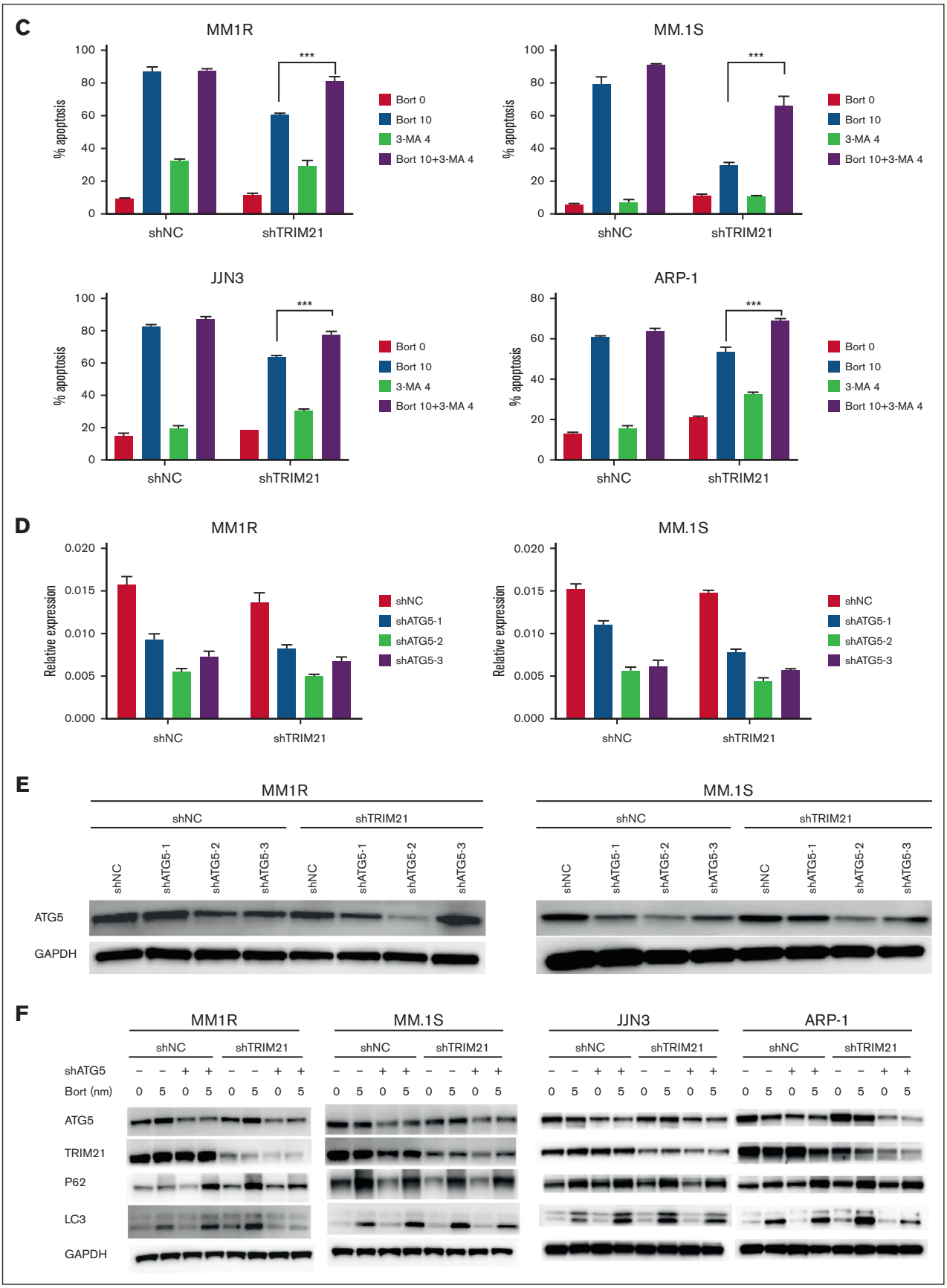

Figure 5 (continued)

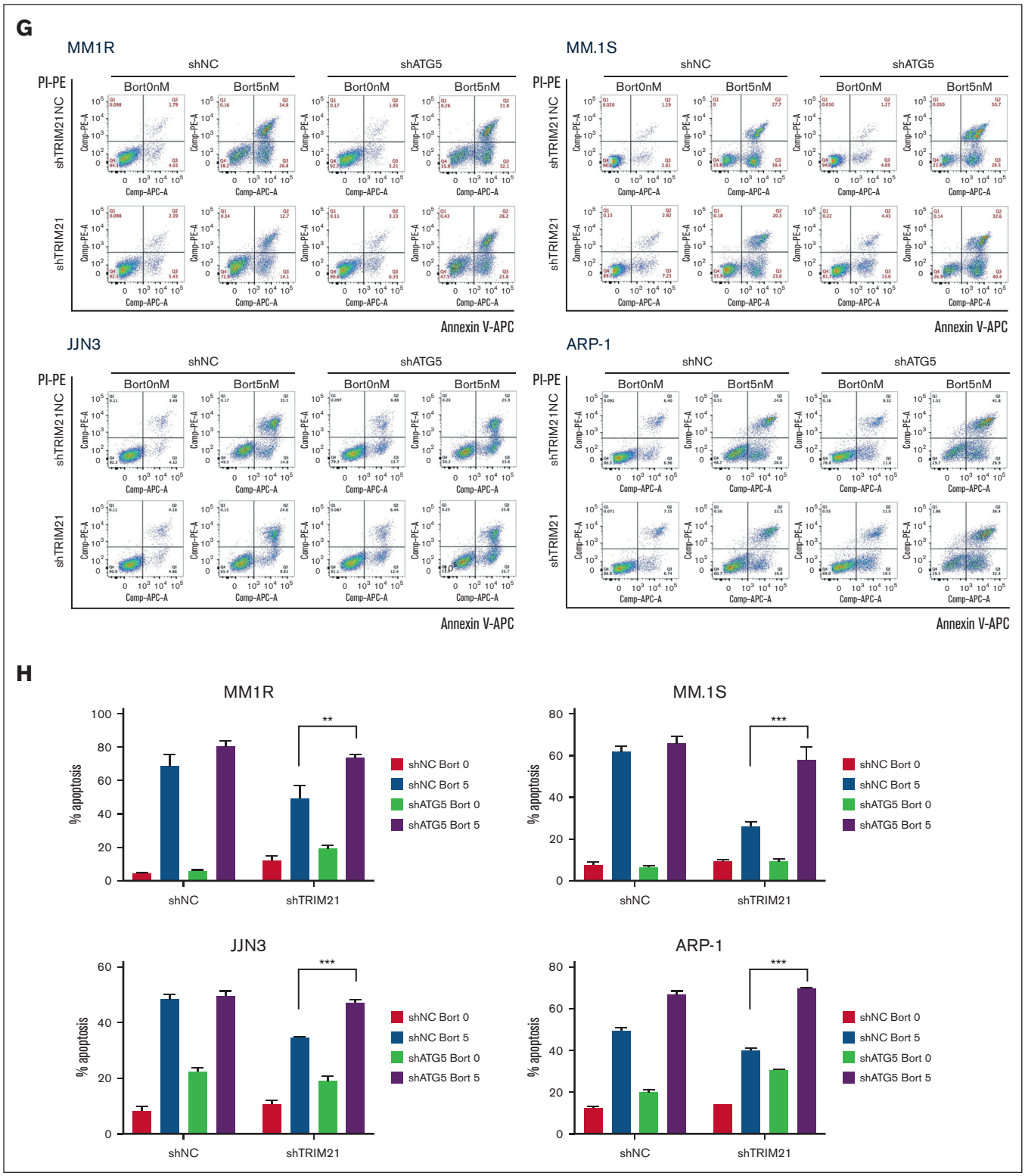

Figure 5 (continued) Inhibition of autophagy restores apoptosis induced by bort. (A) ShTRIM21 or shNC MM1R, MM.1S, JJN3, and ARP-1 cells were incubated with or without 3-MA (4 mM) and bort (5 nM; 24 hours). Western blot analysis was employed to assess LC3 and P62 expression. GAPDH was used as a loading control. (B) Flow cytometry analysis of apoptosis by Annexin-V-APC/PI staining in a representative experiment. (C) The effect of 3-MA in TRIM21-mediated bort resistance is shown as means ± SD. (D) ShTRIM21 or shNC MM1R and MM.1S cells treated with shATG5 (1, 2, 3) compared with shNC showed a remarkable reduction of ATG5 messenger RNA (mRNA) level at 48 hours using qRT-PCR. (E) Western blot assay of ATG5 protein at 48 hours in shTRIM21 or shNC MM1R and MM.1S cells lentivirally transduced with shNC and shATG5 (1, 2, 3).

staining results clearly indicated that compared with the control conditions, TRIM21 OE suppressed LC3-II puncta formation (Figure 4D).

Finally, western blotting revealed that bort reduced pmTOR in both TRIM21 KD and TRIM21 OE MM cell lines. In addition, TRIM21 KD cells had lower levels of pmTOR than the control cells, whereas the TRIM21 OE MM cell lines had relatively higher levels of pmTOR than EV-transfected control cells (Figure 4C). Altogether, our data indicated that TRIM21 KD MM cell lines induced prosurvival autophagy in response to bort treatment.

Autophagy inhibition restores sensitivity to bort in TRIM21 KD MM cells

To assess the role of autophagy in bort-resistant TRIM21 KD MM cells, TRIM21 KD and TRIM21 NC MM1R, MM.1S, JJN3, and ARP-1 cells were treated with the pharmacological autophagy inhibitors 3-MA that blocks the autophagosome formation. As shown in Figure 5A-C, treatment with 3-MA blocked autophagy and induced increased apoptosis in TRIM21 KD MM cells upon bort treatment. By altering the expression of essential ATG5 with shRNAs, the genetic inhibition of autophagy was also performed to analyze the requirement of autophagy in TRIM21 KD MM cells resistant to bort. We designed 3 ATG5 shRNA sequences and choose the "No. 2" sequence in TRIM21 KD and TRIM21 NC MM cells (Figure 5D-E). ShATG5 reduced LC3-II expression, increased P62 degradation, and enhanced bort-induced apoptosis in shTRIM21-MM1R, shTRIM21-MM.1S, shTRIM21-JJN3, and shTRIM21-ARP-1 cells (Figure 5F-H). Taken together, the above data strongly suggest that autophagy plays a role in TRIM21 KD–induced bort resistance.

TRIM21 targets ATG5 directly and mediates ubiquitin-dependent ATG5 degradation in MM cells

ATG5, a component of the ATG12-ATG5 conjugation system in mammals that promotes LC3 conjugation to the nascent autophagic membrane, is essential for the elongation phase of autophagy.[19] To identify the potential interaction partners of TRIM21, and to determine whether the interactions have biological and pathological significance in MM, we characterized the binding of TRIM21 and ATG5 via a coimmunoprecipitation assay. As shown in Figure 6A, ATG5 was present in the TRIM21 complex but not in the immunoglobulin G control, indicating that ATG5 bound to TRIM21. Reciprocally, ATG5 was coimmunoprecipitated with TRIM21 in ARP-1, MM1R, and MM.1S cells (Figure 6B). Next, we performed a GST pulldown assay using purified GST-ATG5 and His-tagged TRIM21. As shown in Figure 6C, ATG5 was associated with purified TRIM21, indicating that ATG5 directly interacted with TRIM21. Moreover, immunofluorescence evaluation in 293T cells revealed colocalization between TRIM21 and ATG5 (Figure 6D).

Considering the role of TRIM21 as an E3 ligase, we conducted a ubiquitination assay to detect whether the effect of TRIM21 on ATG5 was mediated by its ubiquitination activity. For this task, 293T cell lysates were immunoprecipitated with an anti-ATG5 antibody, whereas ATG5 ubiquitination was detected with an antibody against ubiquitin. This experiment demonstrated that in 293T cells, TRIM21 promoted ATG5 ubiquitination through K48 but not K63 conjugation, which contributed to proteasomal degradation (Figure 6E).

In vivo evaluation of TRIM21 potentiates the antimyeloma effect of bort

Finally, we examined the potential antitumor efficacy of TRIM21 in combination with bort using the ARP-1 and JJN3 subcutaneous xenograft nonobese diabetic/severe combined immunodeficiency mouse model. Xenografted mice were randomized to receive phosphate-buffered saline or bort every 3 days by intraperitoneal injection, which led to detectable palpable tumors (~100-130 mm^3). As shown in Figure 7A, the tumor volume measurements revealed that bort treatment significantly inhibited tumor growth from day 12 to day 26 in the ARP-1 subcutaneous xenograft model; in supplemental Figure 4A, the tumor volume in the JJN3 subcutaneous xenograft model was obviously smaller with bort. The mice were euthanized when the volume reached ~3000 mm^3. During the treatment period, a smaller reduction in the tumor growth occurred in the TRIM21 KD group compared with the control group in response to bort treatment, whereas a greater reduction in the TRIM21 OE group than in the control group was observed owing to bort (Figure 7A; supplemental Figure 4A). Consistently, when the mice were euthanized, the tumor size was relatively larger with bort treatment in the TRIM21 KD group with respect to the control group, and as expected, the tumor volumes of TRIM21 OE group were much lower than those in the control group upon bort treatment (Figure 7B; supplemental Figure 4B). We also generated xenograft models via tail vein injection labeled with luciferase into immune-deficient NCG mice to evaluate the role of TRIM21 in MM bort resistance in vivo. Chemiluminescence imaging revealed that in the presence of bort treatment, MM cell bone infiltration and malignant expansion were significantly higher in TRIM21 KD than shNC. Conversely, the OE of TRIM21 significantly suppressed the tumorigenic potential of JJN3 under bort treatment (Figure 7E-F).

To evaluate the effect of combination treatment in vivo, we further performed the immunofluorescence analysis of cleaved Caspase-3 and LC3 staining of tumors harvested from mice undergoing different treatments. As shown in Figure 7C, the number of TRIM21 and cleaved Caspase-3 positive MM cells in the TRIM21 KD group was significantly decreased as compared with the control group upon bort treatment. A significant increase in ATG5 and LC3 expression was also noted in tumor sections from the TRIM21 KD group compared with the control group in response to bort. Simultaneously, TRIM21-repressed tumors exhibited more positive staining of TRIM21 and cleaved Caspase-3, yet more negative staining of ATG5 and LC3 (Figure 7D). Overall, these experiments validated the in vitro observations and demonstrated the efficacy of TRIM21 in inducing apoptosis and inhibiting antophagy to enhance the in vivo anti-MM activity of bort.

Figure 5 (continued) GAPDH was used as a loading control. (F) Western blot analysis of the effect of shATG5 on LC3 and P62 expression in shNC or shTRIM21 MM1R, MM.1S, JJN3, and ARP-1 cells in the absence or presence of bort (5 nM; 24 hours). (G) Effect of bort (5 nM; 24 hours) on apoptosis in shTRIM21 or shNC MM1R, MM.1S, JJN3, and ARP-1 cells according to a representative flow cytometry experiment after ATG5 shRNA treatment. Notably, ATG5 KD–induced apoptosis. (H) The effect of shATG5 in TRIM21-mediated bort resistance is shown as means ± SD. The values are presented as the mean ± SD of 3 independent experiments. (*$P < .05$; **$P < .01$; ***$P < .001$).

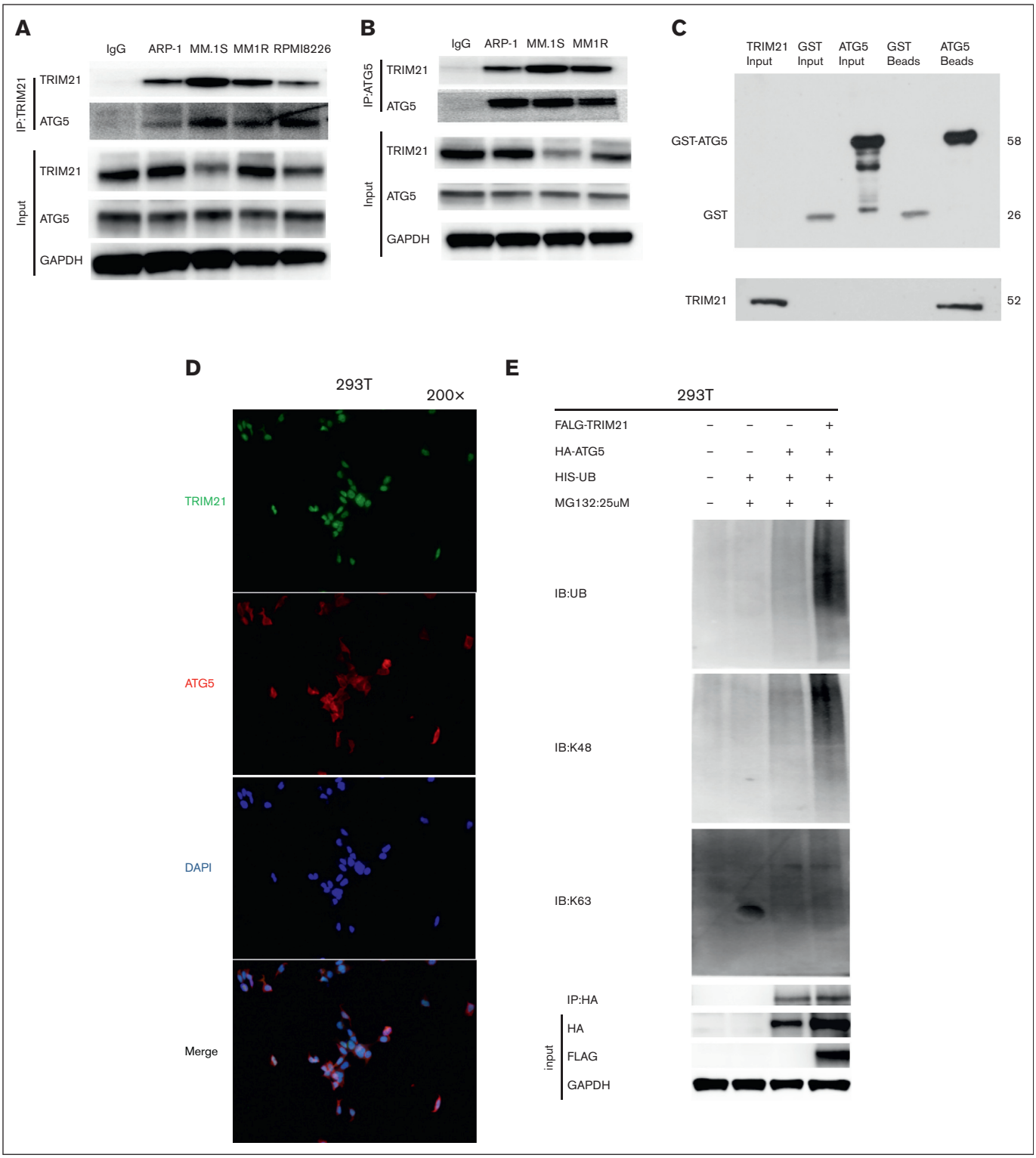

Figure 6. TRIM21 targets ATG5 directly and regulates ATG5 ubiquitination. (A) TRIM21 immunoprecipitated endogenous ATG5. ARP-1, MM.1S, MM1R, and RPMI8226 cell extracts were immunoprecipitated with an antibody against ATG5, along with the immunoglobulin G (IgG) control, followed by western blotting with an ATG5 antibody. (B) ATG5 immunoprecipitated endogenous TRIM21. ARP-1, MM.1S, and MM1R cells were lysed and immunoprecipitated with an ATG5 antibody, followed by incubation with TRIM21. (C) The GST-pull down test showed that ATG5 was directly bound to TRIM21. The GST-ATG5 fusion protein was ~58 kDa in size. The HIS-TRIM21 protein was ~52 kDa in size. We detected HIS-TRIM21 in the supernatant of bacterial lysates and in the supernatant of GST-ATG5 beads. GST alone was used as a negative control. GST-ATG5 and HIS-TRIM21 were purified from *Escherichia coli*. (D) Immunofluorescence staining assay showing TRIM21 and ATG5 subcellular colocalization in 293T cells. The nuclei were stained with 4′,6-diamidino-2-phenylindole (DAPI). Original magnification: 200×, scale bar: 100 μm. (E) TRIM21 OE 293T cells were treated with MG-132 (25 μm; 6

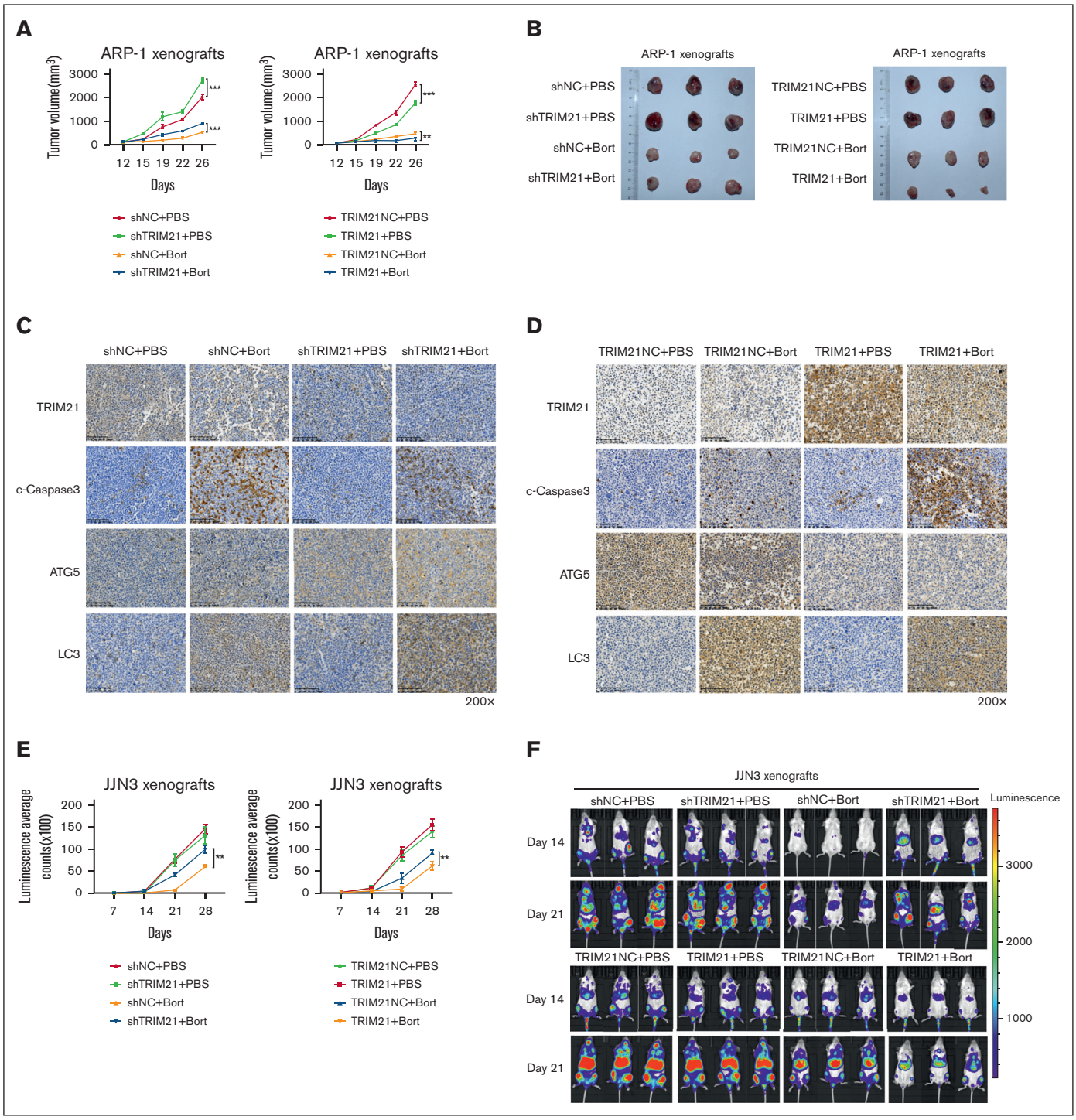

Figure 7. In vivo evaluation of TRIM21 potentiates the antimyeloma effect of bort. A total of 5 × 10^6 TRIM21 KD or OE ARP-1 cells were subcutaneously injected into nonobese diabetic (NOD)-severe combined immunodeficiency (SCID) mice (n = 24). The tumor size was measured with a caliper, and PBS or bort (0.5 mg/kg) was injected every 3 to 4 days when the established tumors reached ~100 to 130 mm^3 on day 12. (A) Tumor volume of each group shown as mean ± SD. (B) Xenografts were excised and photographed on day 26. (C-D) Immunohistochemistry analysis of TRIM21, ATG-5, c-Caspase-3, and LC3 on tumor tissue sections from each group. Summary measurement of signals (E) and representative images of chemiluminescence (F) in the TRIM21 KD, TRIM21 OE and control group. Original magnification: 200×. Scale bars: 100 μm. (*$P < .05$; **$P < .01$; ***$P < .001$).

Figure 6 (continued) hours) and the whole-cell lysates (WCLs) were then collected for the detection of FLAG-TRIM21, HA-ATG5, and GAPDH protein levels by immunoblotting. The WCLs were subjected to IP using an anti-ATG5 antibody, and ubiquitinated ATG5 was evaluated with a related ubiquitin antibody.

Discussion

TRIM21 is a well-known target of circulating autoantibodies and thus plays a major role in immune signaling and autoimmune disease.[20-22] TRIM21 possesses E3 ligase activity, and recent studies have shown that it participates in drug resistance via regulating the turnover of specific substrates. In acute myeloid leukemia cells, TRIM21 can increase the ubiquitination level of the histone methyltransferase EZH2 and reduce its sensitivity to drugs.[23] In human pancreatic cancer, TRIM21 expression is significantly increased in gemcitabine-resistant cells.[24] TRIM12 also improves the chemosensitivity of gastric cancer cells to apatinib treatment through the reduction of EZH1 levels.[25] Therefore, researchers believe that interactions between TRIM21 and its specific substrates have important functional consequences in cancers.[26,27] The *TRIM21* gene is located in the tumor suppressor locus on the short arm of chromosome 11, which is associated with MM. Nonetheless, the direct substrates and additional roles of TRIM21 remain unknown. To this end, we initiated this study to find that low TRIM21 expression is a relapsing factor for MM. Our in vitro and in vivo experiments both evidenced that TRIM21 OE sensitizes MM cells to bort, suggesting that TRIM21 may be a potential target to overcome bort resistance in MM cells.

Normal plasma cells maintain cellular energy balance by autophagy, a mechanism to regulate endoplasmic reticulum stress and immunoglobulin secretion.[28,29] In addition, various forms of endoplasmic reticulum stress trigger autophagy by activating unfolded protein responses.[30,31] Regarding MM, different from normal plasma cells, aberrant plasma cells undergo unfolded protein response–dependent autophagy.[12,32-34] Hoang et al found that autophagy inhibition effect of pharmacological drugs or silencing the ATG expression led to myeloma cell death.[35] In some cases, excessive autophagy activation causes excessive organelle elimination and ultimately results in autophagic cell death.[36] Laurence et al have delineated that MM cells balance the prosurvival and prodeath effects of autophagy through a heterodimeric protease consisting of caspase-10 and $cFLIP_L$.[37] Hence, we speculated that TRIM21, as an ATG, might inhibit protective autophagy in MM cells under bort treatment. Furthermore, we indicated that the TRIM21 KD in MM reduces bort sensitivity, and these effects are mediated through proautophagy pathway activation. We restored MM sensitivity to bort by suppressing autophagosome formation using autophagy inhibitors, such as 3-MA or ATG5 silencing in TRIM21 KD MM cells.

Our findings have significant clinical implications. Bort as a proteasome inhibitor has been commonly used as first-line treatment for patients with MM. However, with the increasingly frequent clinical use of bort, patients develop drug resistance and recurrence, ultimately reducing the efficacy of this agent.[38-40] Therefore, it remains urgent to explore pathways to increase drug sensitivity or prevent the development of drug resistance. In this study, we described the role TRIM21 plays in the response of MM cells to bort, and found that TRIM21 OE increases the cytotoxicity of bort in MM cells in vitro. Mechanistically, TRIM21 can inhibit autophagy by ubiquitinating the key gene ATG5 in autophagosome formation, which in turn leads to increased cell death.

Overall, our investigation elucidates the key role of TRIM21 in bort resistance in MM cells. The E3 ligase TRIM21 acts by targeting ATG5 to inhibit autophagy and enhance MM cell death, thus providing the basis for a novel therapeutic approach and opportunities to develop drugs targeting autophagy. In the treatment of cancer, including MM, autophagy inhibitors are being considered for preclinical and ongoing clinical studies.[41-43] Notably, we need to be careful in considering the use of classical autophagy inhibitors to block autophagy because all cells maintain a basic level of autophagy that increases with adaptive responses to cell survival or death. For patients with low TRIM21 expression, a combination of autophagy inhibitors may consist a viable option to enhance the effect of bort in MM treatment.

Acknowledgments

The authors appreciate all the staff of the Zhejiang University School of Medicine and thank Xiaojian Wang for guiding the experiments.

This work was supported by the National Natural Science Foundation of China (project nos. 81900209, 81872322, 81800202), Zhejiang Key Research and Development Project (2020C03014).

Authorship

Contribution: J.C., L.Y., and Z.C. initiated and designed the study; J.C. and W.C. performed the majority of the experiments; J.C. wrote the manuscript; X.H., Q.C., S. Ye, J.Q., Y.L., X.G., S. Yao, and E.Z. performed the research and analyzed the data; J.H. and A.L. collected primary samples for the study; and L.Y. and Z.C. supervised the experiments.

Conflict-of-interest disclosure: The anthors declare no competing financial interests.

ORCID profile: Z.C., 0000-0001-6026-3804.

Correspondence: Zhen Cai, Bone Marrow Transplantation Center, The First Affiliated Hospital, School of Medicine, Zhejiang University, No 79, Qingchun Rd, Hangzhou 310003, China; Institute of Hematology, Zhejiang University, Hangzhou, 310003, China; email: caiz@zju.edu.cn; and Li Yang, Bone Marrow Transplantation Center, The First Affiliated Hospital, School of Medicine, Zhejiang University, No 79, Qingchun Rd, Hangzhou 310003, China; email: liyanghz@zju.edu.cn.

References

1. Waldschmidt JM, Yee AJ, Vijaykumar T, et al. Cell-free DNA for the detection of emerging treatment failure in relapsed/refractory multiple myeloma. *Leukemia*. 2022;36(4):1078-1087.

2. Kastritis E, Terpos E, Dimopoulos MA. How I treat relapsed multiple myeloma. *Blood*. 2022;139(19):2904-2917.

3. Franke NE, Niewerth D, Assaraf YG, et al. Impaired bortezomib binding to mutant beta5 subunit of the proteasome is the underlying basis for bortezomib resistance in leukemia cells. *Leukemia*. 2012;26(4):757-768.
4. Rastgoo N, Pourabdollah M, Abdi J, Reece D, Chang H. Dysregulation of EZH2/miR-138 axis contributes to drug resistance in multiple myeloma by downregulating RBPMS. *Leukemia*. 2018;32(11):2471-2482.
5. Zhang L, Rastgoo N, Wu J, et al. MARCKS inhibition cooperates with autophagy antagonists to potentiate the effect of standard therapy against drug-resistant multiple myeloma. *Cancer Lett*. 2020;480:29-38.
6. Podar K, Chauhan D, Anderson KC. Bone marrow microenvironment and the identification of new targets for myeloma therapy. *Leukemia*. 2009;23(1):10-24.
7. Robak P, Drozdz I, Szemraj J, Robak T. Drug resistance in multiple myeloma. *Cancer Treat Rev*. 2018;70:199-208.
8. Levine B, Kroemer G. Autophagy in the pathogenesis of disease. *Cell*. 2008;132(1):27-42.
9. Shintani T, Klionsky DJ. Autophagy in health and disease: a double-edged sword. *Science*. 2004;306(5698):990-995.
10. Chung C, Seo W, Silwal P, Jo EK. Crosstalks between inflammasome and autophagy in cancer. *J Hematol Oncol*. 2020;13(1):100.
11. de Campos CB, Zhu YX, Sepetov N, et al. Identification of PIKfyve kinase as a target in multiple myeloma. *Haematologica*. 2019;105(6):1641-1649.
12. Zheng Z, Wang L, Cheng S, Wang Y, Zhao W. Autophagy and myeloma. *Adv Exp Med Biol*. 2020;1207:625-631.
13. Feng Y, He D, Yao Z, Klionsky DJ. The machinery of macroautophagy. *Cell Res*. 2014;24(1):24-41.
14. Platta HW, Abrahamsen H, Thoresen SB, Stenmark H. Nedd4-dependent lysine-11-linked polyubiquitination of the tumour suppressor Beclin 1. *Biochem J*. 2012;441(1):399-406.
15. Shi CS, Kehrl JH. TRAF6 and A20 regulate lysine 63-linked ubiquitination of Beclin-1 to control TLR4-induced autophagy. *Sci Signal*. 2010;3(123):ra42.
16. Sui B, Wang M, Cheng C, et al. Nanogel-facilitated protein intracellular specific degradation through Trim-away. *Adv Funct Mater*. 2021;31(30):2010556.
17. Niida M, Tanaka M, Kamitani T. Downregulation of active IKK beta by Ro52-mediated autophagy. *Mol Immunol*. 2010;47(14):2378-2387.
18. Kimura T, Jain A, Choi SW, et al. TRIM-mediated precision autophagy targets cytoplasmic regulators of innate immunity. *J Cell Biol*. 2015;210(6):973-989.
19. Xie Y, Kang R, Sun X, et al. Posttranslational modification of autophagy-related proteins in macroautophagy. *Autophagy*. 2015;11(1):28-45.
20. Fletcher AJ, James LC. Coordinated neutralization and immune activation by the cytosolic antibody receptor TRIM21. *J Virol*. 2016;90(10):4856-4859.
21. Lee AYS. A review of the role and clinical utility of anti-Ro52/TRIM21 in systemic autoimmunity. *Rheumatol Int*. 2017;37(8):1323-1333.
22. Gao W, Li Y, Liu X, et al. TRIM21 regulates pyroptotic cell death by promoting Gasdermin D oligomerization. *Cell Death Differ*. 2022;29(2):439-450.
23. Gollner S, Oellerich T, Agrawal-Singh S, et al. Loss of the histone methyltransferase EZH2 induces resistance to multiple drugs in acute myeloid leukemia. *Nat Med*. 2017;23(1):69-78.
24. Shen Y, Pan Y, Xu L, et al. Identifying microRNA-mRNA regulatory network in gemcitabine-resistant cells derived from human pancreatic cancer cells. *Tumour Biol*. 2015;36(6):4525-4534.
25. Ping M, Wang S, Guo Y, Jia J. TRIM21 improves apatinib treatment in gastric cancer through suppressing EZH1 stability. *Biochem Biophys Res Commun*. 2022;586:177-184.
26. Qin B, Zou S, Li K, et al. CSN6-TRIM21 axis instigates cancer stemness during tumorigenesis. *Br J Cancer*. 2020;122(11):1673-1685.
27. Su X, Feng C, Wang S, et al. The noncoding RNAs SNORD50A and SNORD50B-mediated TRIM21-GMPS interaction promotes the growth of p53 wild-type breast cancers by degrading p53. *Cell Death Differ*. 2021;28(8):2450-2464.
28. Pengo N, Scolari M, Oliva L, et al. Plasma cells require autophagy for sustainable immunoglobulin production. *Nat Immunol*. 2013;14(3):298-305.
29. Parzych KR, Klionsky DJ. An overview of autophagy: morphology, mechanism, and regulation. *Antioxid Redox Signal*. 2014;20(3):460-473.
30. Hetz C, Glimcher LH. Fine-tuning of the unfolded protein response: assembling the IRE1alpha interactome. *Mol Cell*. 2009;35(5):551-561.
31. Ravanan P, Srikumar IF, Talwar P. Autophagy: the spotlight for cellular stress responses. *Life Sci*. 2017;188:53-67.
32. Kunjom Mfopou J, Bouwens L. [Differentiation of pluripotent stem cells into pancreatic lineages]. *Med Sci (Paris)*. 2013;29(8-9):736-743.
33. Yun Z, Zhichao J, Hao Y, et al. Targeting autophagy in multiple myeloma. *Leuk Res*. 2017;59:97-104.
34. Desantis V, Saltarella I, Lamanuzzi A, et al. Autophagy: a new mechanism of prosurvival and drug resistance in multiple myeloma. *Transl Oncol*. 2018;11(6):1350-1357.
35. Hoang B, Benavides A, Shi Y, Frost P, Lichtenstein A. Effect of autophagy on multiple myeloma cell viability. *Mol Cancer Ther*. 2009;8(7):1974-1984.
36. Galluzzi L, Vitale I, Abrams JM, et al. Molecular definitions of cell death subroutines: recommendations of the Nomenclature Committee on Cell Death 2012. *Cell Death Differ*. 2012;19(1):107-120.
37. Lamy L, Ngo VN, Emre NC, et al. Control of autophagic cell death by caspase-10 in multiple myeloma. *Cancer Cell*. 2013;23(4):435-449.
38. Tian Z, D'Arcy P, Wang X, et al. A novel small molecule inhibitor of deubiquitylating enzyme USP14 and UCHL5 induces apoptosis in multiple myeloma and overcomes bortezomib resistance. *Blood*. 2014;123(5):706-716.

39. Song Y, Li S, Ray A, et al. Blockade of deubiquitylating enzyme Rpn11 triggers apoptosis in multiple myeloma cells and overcomes bortezomib resistance. *Oncogene*. 2017;36(40):5631-5638.

40. Wallington-Beddoe CT, Sobieraj-Teague M, Kuss BJ, Pitson SM. Resistance to proteasome inhibitors and other targeted therapies in myeloma. *Br J Haematol*. 2018;182(1):11-28.

41. Frassanito MA, De Veirman K, Desantis V, et al. Halting pro-survival autophagy by TGFbeta inhibition in bone marrow fibroblasts overcomes bortezomib resistance in multiple myeloma patients. *Leukemia*. 2016;30(3):640-648.

42. Scott EC, Maziarz RT, Spurgeon SE, et al. Double autophagy stimulation using chemotherapy and mTOR inhibition combined with hydroxychloroquine for autophagy modulation in patients with relapsed or refractory multiple myeloma. *Haematologica*. 2017;102(7):e261-e265.

43. Vogl DT, Stadtmauer EA, Tan KS, et al. Combined autophagy and proteasome inhibition: a phase 1 trial of hydroxychloroquine and bortezomib in patients with relapsed/refractory myeloma. *Autophagy*. 2014;10(8):1380-1390.